

A structural approach by MAS NMR spectroscopy of mechanisms occurring under β -irradiation in mixed alkali aluminoborosilicate glasses

This article has been downloaded from IOPscience. Please scroll down to see the full text article.

2004 J. Phys.: Condens. Matter 16 7625

(<http://iopscience.iop.org/0953-8984/16/43/006>)

View [the table of contents for this issue](#), or go to the [journal homepage](#) for more

Download details:

IP Address: 129.252.86.83

The article was downloaded on 27/05/2010 at 18:23

Please note that [terms and conditions apply](#).

A structural approach by MAS NMR spectroscopy of mechanisms occurring under β -irradiation in mixed alkali aluminoborosilicate glasses

N Ollier¹, T Charpentier², B Boizot¹ and G Petite¹

¹ Laboratoire des Solides Irradiés, UMR 7642 CEA-CNRS-Ecole Polytechnique, Ecole Polytechnique, 91128 Palaiseau Cedex, France

² Service de Chimie Moléculaire, DSM/DRECAM/ CEA Saclay, 91191 Gif-sur-Yvette Cedex, France

Received 8 July 2004, in final form 9 September 2004

Published 15 October 2004

Online at stacks.iop.org/JPhysCM/16/7625

doi:10.1088/0953-8984/16/43/006

Abstract

Two series of mixed Na/K and Na/Li aluminoborosilicate glasses have been irradiated with electrons of 1.8 MeV at doses close to 10^9 Gy. Si, B and Al glass former environment changes under irradiation have been probed by MAS NMR spectroscopy. It was shown that the mixed alkali effect acts on the middle range compositions by operating with a selective blockage in irradiated glasses, depending on the alkali nature and concerning either modifier or charge compensator alkalis.

1. Introduction

Irradiation effects on glasses have been studied for a long time, especially in links with high-level nuclear waste glass disposal. Under alpha, beta and gamma radiations, macroscopic changes occur like positive or negative volume changes; mechanical properties such as hardness and fracture toughness are also affected [1, 2]. Concerning microscopic changes, it has been shown by transmission electron microscopy (TEM) that gas bubbles can be formed [3, 4], as well as glass demixing which can occur [4, 5]. Under sufficient β irradiation dose, Boizot *et al* [6] demonstrated that most of the structural modifications in borosilicate glasses (polymerization increase and molecular oxygen formation) were connected to the alkali migration. By studying more complex glass compositions close to the French Nuclear glass SON68, we observed that structural changes were less pronounced [7]. So our approach is the following: the glass compositions are made more complex stepwise in order to analyse the influence of each added product. On one hand, addition of iron in the matrix was found to notably reduce the concentration of paramagnetic point defects created under irradiation [8]. On the other hand, the mixed alkali effect (MAE) is well known to decrease considerably the alkali motions, the largest effect being often observed by mixing two alkalis in equal

Table 1. Nominal glass compositions in mol%; a = Na₂O/Na₂O + K₂O and b = Na₂O/Na₂O + Li₂O.

mol%	5Ox– 0K(0Li)	5Ox– 25K	5Ox– 40K	5Ox– 50K	5Ox– 60K	5Ox– 75K	5Ox– 100K	5Ox– 25Li	5Ox– 50Li	5Ox– 75Li	5Ox– 100Li
a	1.00	0.75	0.60	0.50	0.40	0.25	0.00				
b								0.75	0.50	0.25	0.00
SiO ₂	63.47	63.47	63.47	63.47	63.47	63.47	63.47	63.47	63.47	63.47	63.47
Al ₂ O ₃	4.04	4.04	4.04	4.04	4.04	4.04	4.04	4.04	4.04	4.04	4.04
B ₂ O ₃	16.80	16.80	16.80	16.80	16.80	16.80	16.80	16.80	16.80	16.80	16.80
Na ₂ O	13.34	10.01	8.00	6.67	5.34	3.34		10.01	6.67	3.34	
ZrO ₂	2.35	2.35	2.35	2.35	2.35	2.35	2.35	2.35	2.35	2.35	2.35
K ₂ O		3.34	5.34	6.67	8.00	10.01	13.34				
Li ₂ O								3.34	6.67	10.01	13.34

concentration. One good illustration is the significant decrease of the ionic conductivity (four or five decades lower than for the single composition) [9–11]. Thus, we wanted to check if the MAE can cause the reduction of alkali migration under irradiation. Indeed, our preliminary results on Na/K and Na/Li glasses have shown that MAE can limit some structural changes under irradiation whose origin is assigned to alkaline migration [12]. Polymerization increase and defect formation were minimized for the 50/50 Na/Li irradiated glass, whereas a different behaviour was observed for the 50/50 Na/K glass [12]. The present study is realized on the same two glass series by magic angle spinning nuclear magnetic resonance (MAS NMR) spectroscopy on ²⁹Si, ¹¹B and ²⁷Al nuclei. It is therefore more dedicated to the analysis of local order changes around glass formers and to the understanding of the observed differences between Na/Li and Na/K glasses [12].

2. Experimental part

Two glass series were synthesized mixing two alkali ions (Na with Li and Na with K) within a range of different molar ratios. All glasses were prepared by adding stoichiometric amounts of SiO₂, H₃BO₃, Na₂CO₃, K₂CO₃, Li₂CO₃, Al₂O₃ and ZrO₂. For Na/K glasses, the dried mixed powders were first heated at 750 °C in a Pt crucible for 10 h for decarbonation. Then, the mixture was melted at 1500 °C for 1 h and quenched in air. The glass was annealed at 500 °C for 1 h to release strains. For Na/Li glasses, powders were melted at 1400 °C in a Pt crucible and annealed at 520 °C in a graphite crucible for 1 h. Each glass was analysed by x-ray diffraction, which confirmed its amorphous character. Nominal glass compositions are displayed in table 1 (in mol%). The glass name (first line of the table) is linked to its composition as follows: 5Ox–75Li indicates a 5 oxide glass with 75% of Li₂O (mol%).

5 mm by 5 mm glass plates were irradiated with 1.8 MeV electrons provided by the LSI Van de Graaff accelerator. Glass thickness is limited to 600 μm to allow a homogeneous irradiation in the glass volume. For NMR experiments, about 50 mg of massive glass was irradiated before being ground. A 10⁹ Gy irradiation dose was reached on each sample using a 20 μA beam; the sample temperature was maintained at 30 °C.

Raman spectra were collected with a Labram HR micro-spectrometer using the 514.5 nm line of an Ar⁺ laser. Experiments were carried out through a ×100 Olympus objective; the measured power was 17 mW at the sample.

²⁹Si and ¹¹B MAS NMR spectra of powder glasses were collected on a Bruker AVANCE 500 spectrometer operating at a Larmor frequency of 99.71 and 160.14 MHz, respectively. A 4 mm o.d. Bruker MAS probe was used and sample-spinning speed was 12 500 Hz.

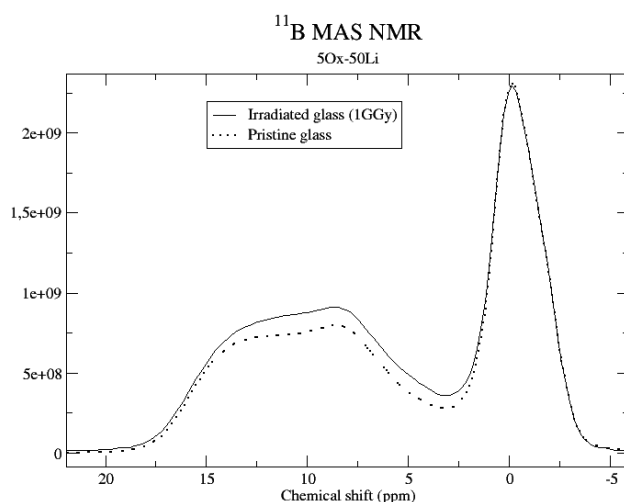


Figure 1. ^{11}B MAS NMR spectra of 50x–50Li irradiated and non-irradiated glasses.

^{29}Si MAS spectra were accumulated (typically 4000 scans) using a recycle delay of 20 s and a 90° pulse length of $4\ \mu\text{s}$. The choice of a 20 s recycle delay is based on several measurements up to 120 s and on the knowledge of the presence of a small amount of Fe^{3+} detected by electron paramagnetic resonance spectroscopy which reduces the ^{29}Si relaxation time. ^{11}B MAS NMR spectra were collected using a recycle delay of 2 s and a pulse length of $1\ \mu\text{s}$ in order to obtain quantitative spectra. ^{29}Si and ^{11}B chemical shifts are reported in ppm and are referenced to an external sample of TKS (-9.8 , -135 ppm) and to 1 M boric acid (19.6 ppm), respectively.

^{27}Al MAS NMR spectra of powder samples were acquired on both a Bruker AVANCE 500 spectrometer operating at a Larmor frequency of 130.06 MHz and a Bruker AVANCE 300 operating at a Larmor frequency of 78.20 MHz. A Bruker MAS probe with 4 mm rotor was used and sample spinning speed was 14 kHz. For MAS spectra, up to 512 free induction decays were accumulated with single-pulse excitation of length $1\ \mu\text{s}$ and recycle delay of 1 s in order to obtain quantitative spectra. MQ-MAS spectra were acquired using a Z filter sequence [13]. ^{27}Al NMR frequencies were externally calibrated against a 1 M $\text{Al}(\text{Cl})_3$ solution. Data were processed and fitted using a homebuilt program.

3. Results

3.1. Boron environment

^{11}B MAS NMR spectra were recorded for the Na, Li, K and the 50/50 Na/Li and Na/K irradiated glass compositions and compared to the non-irradiated samples.

^{11}B MAS NMR spectra of both glass series consist of two lines centred at 0 and 11 ppm, corresponding respectively to BO_4 and BO_3 species [14] (see figure 1 corresponding to the intermediate irradiated and non-irradiated Na/Li glass). On the normalized 50x–50Li irradiated glass spectrum (figure 1), an increase of BO_3 species (or inversely a decrease of BO_4 species) takes place, implying a conversion of BO_4 into BO_3 species under irradiation. A similar phenomenon is observed on single-alkali glasses 50x–100Li, 50x–0K and 50x–100K displayed in figure 2. In contrast, 50x–50K irradiated and non-irradiated glasses exhibit the

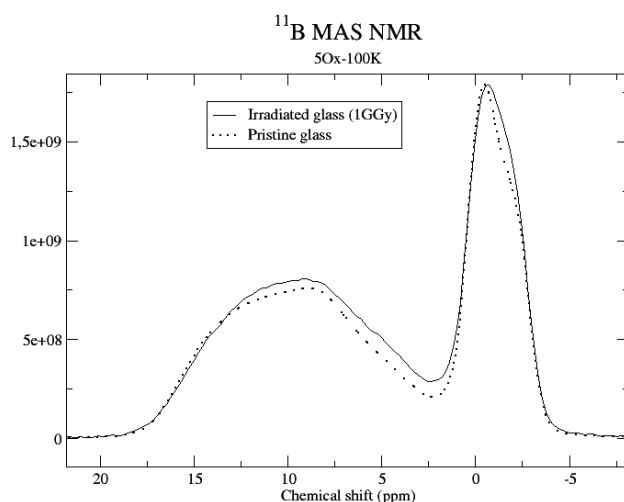


Figure 2. ^{11}B MAS NMR spectra of 50x–100K irradiated and non-irradiated glasses.

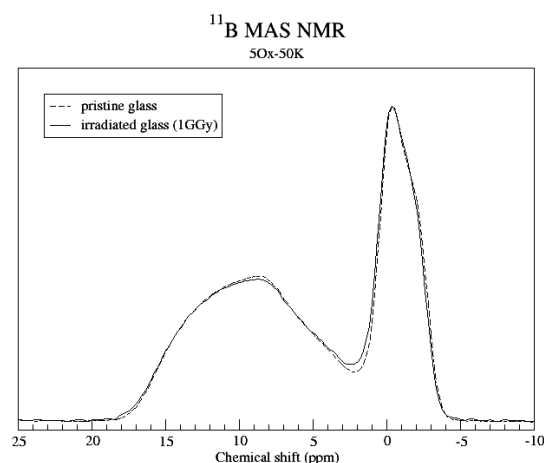


Figure 3. ^{11}B MAS NMR spectra of 50x–50K irradiated and non-irradiated glasses.

same ^{11}B MAS NMR spectrum, indicating that the BO_4/BO_3 ratio is stable after irradiation (figure 3). Concerning the K glass, we can observe moreover that the BO_4 and BO_3 lines are modified under irradiation (figure 2). In one of our recent papers [15], we reported results concerning Na/K and Na/Li glass structure and more particularly the identification of boron sites by ^{11}B multi-quantum magic angle spinning. Two different BO_4 sites were clearly detected as well as both BO_3 sites which were attributed to ring and non-ring components. We evaluated the boron conversion rate from a careful ^{11}B fit procedure described in [15]. It can be extracted from the deconvolution that the BO_3 species increases by 7% after irradiation in 50x–50Li glass, 4% in 50x–100Li glass, 3% in 50x–0K and more slightly in 50x–100K glass (about 2%). Concerning species repartition, an estimation of the non-ring species can be proposed: it increases by 25% in K and Li glasses; this change is limited in 50x–50Li glass. A more precise measurement needs further developments for MQ-MAS spectrum interpretation that is on the way.

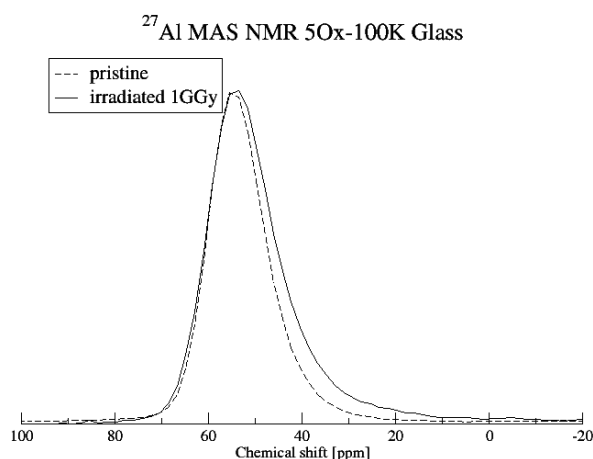


Figure 4. ^{27}Al MAS NMR spectra of 50x–100K irradiated and non-irradiated glasses.

3.2. Aluminium environment

^{27}Al MAS NMR spectra of the 50x–100K glasses (irradiated and not) are displayed in figure 4. Each spectrum contains a single broad peak in the chemical shift region 40–70 ppm, corresponding to aluminium under fourfold coordination [16]. The asymmetric line-shape of the MAS spectrum is due to a distribution of both the quadrupolar interaction and isotropic chemical shift. The centre of gravity of a MAS spectrum is given by

$$\delta_{\text{MAS}} = \delta_{\text{iso}} + \delta_{\text{QIS}}^{(2)},$$

$$\delta_{\text{QIS}}^{(2)} = \frac{-3 P_{\text{Q}}^2 I(I+1) - 3/4}{40 \nu_0^2 I^2(2I-1)^2} \quad \text{and} \quad P_{\text{Q}}^2 = C_{\text{Q}}^2(1 + \eta^2/3)$$

where δ_{iso} is the average isotropic chemical shift, $\delta_{\text{QIS}}^{(2)}$ the average second order quadrupolar induced shift, ν_0 is the Larmor frequency, C_{Q} the quadrupolar coupling constant and η the asymmetry parameter of the quadrupolar interaction.

From MAS spectra at two fields (here 7.05 and 11.75 T), average values of δ_{iso} and P_{Q} can be extracted for all glasses. This method has already been successfully applied for ^{23}Na ; see for example [19]. In figure 5, the variation of P_{Q} is plotted as a function of the alkali Na/Li and Na/K ratios. Two different variation trends can be observed according to the glass compositions. For the Na/Li series, P_{Q} follows a linear increase when Li is progressively substituted by Na. For the Na/K series, the variation is constituted by two modes: a flat part until the 40% Na_2O , 60% K_2O glass composition followed by a decreasing part (dotted line). Such a behaviour can be interpreted in terms of aluminium charge compensators. Na^+ cations seem to preferentially compensate the AlO_4^- entities against K. Moreover, we can remark that $P_{\text{Q}}(\text{Li}) \geq P_{\text{Q}}(\text{Na}) \geq P_{\text{Q}}(\text{K})$. This variation is consistent with the FWHM of the MAS spectra and indicates a much more aluminium distorted environment for the Li glass than the K one.

Figure 4 also shows that the full width at half maximum (FWHM) of the ^{27}Al line increases after irradiation. This is consistent with the MQ-MAS data as discussed below. This behaviour is general and concerns all glass compositions; however, we may notice that the aluminium speciation is stable under irradiation (for dose of 10^9 Gy) in contrast to boron.

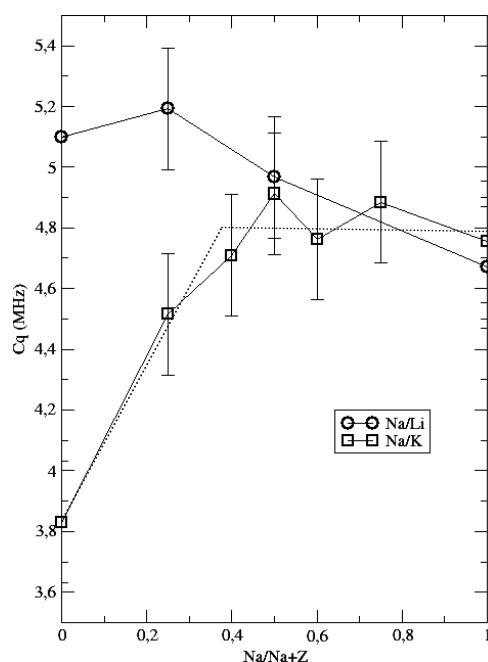


Figure 5. Quadrupolar coupling constant (C_Q) as a function of $\text{Na}/\text{Na} + \text{Z}$; $\text{Z} = \text{Li}$ for the circles and $\text{Z} = \text{K}$ for the squares.

3.3. Silicon environment

^{29}Si MAS NMR spectra of 50x–50Li and 50x–100Li irradiated and non-irradiated glasses are exhibited in figures 6(a) and 7(a) respectively. A strong shift of the ^{29}Si line between pristine and irradiated glass is visible in 50x–100Li glass. The gravity centre position shifts from -99.3 ppm (pristine glass) to -103 ppm (irradiated). For 50x–50Li, the ^{29}Si band shift is nearly imperceptible, consistent with the constant value of the gravity centre of the ^{29}Si line. Each NMR spectrum is associated with the corresponding Raman spectrum shown in part B (figures 6 and 7). Raman bands attributed to Q^3 and Q^2 species are found respectively at 1100 and 980 cm^{-1} (the Q^n denomination corresponds to SiO_4 species with n bridging oxygens) [18]. We can observe in one case that the Q^3/Q^2 ratio increases after irradiation (50x–50K), whereas for the 50x–50Li glass the Q^3/Q^2 ratio is kept constant after irradiation.

4. Discussion

By analysing several compositions of glasses along two mixed alkali series (Na/Li and Na/K), we demonstrate different behaviours under irradiation. We try first to establish relationships between all structural changes observed by Raman and NMR spectroscopy.

4.1. Molecular oxygen

The first point concerns molecular oxygen formation: the non-detection of molecular oxygen in irradiated glasses containing more than 50% of K (whereas a polymerization increase was attested by Raman spectroscopy) constituted one of the remaining unclear points in our previous paper [12]. It was previously shown that in a Na borosilicate the conversion of BO_4 into

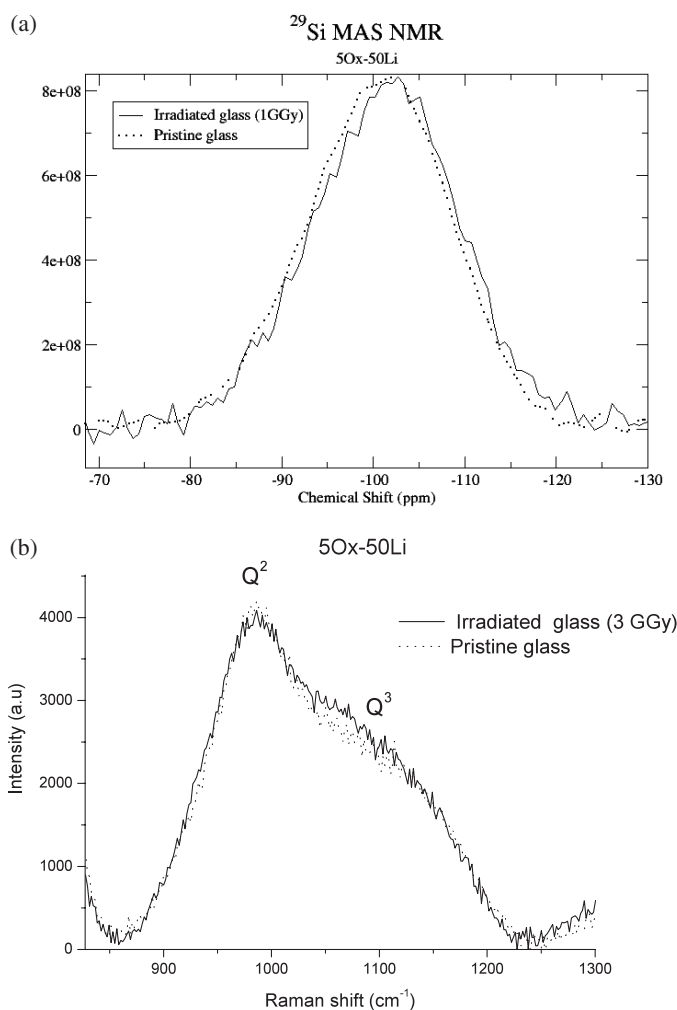


Figure 6. (a) ^{29}Si MAS NMR spectra of 50x-50Li irradiated and non-irradiated glasses. (b) Raman spectra of 50x-50Li irradiated and non-irradiated glasses.

BO_3 species contributes to the formation of molecular oxygen as well as the polymerization increase [6].

Thanks to ^{11}B MAS NMR spectroscopy, we detected that conversion of BO_4 into BO_3 does not occur systematically in our irradiated glasses; see for example the 50x-50K sample (figure 3). It is worth mentioning that the equivalent Na/Li composition (50x-50Li glass) exhibits a contrary behaviour with 7% of BO_4 species converted into BO_3 species. These results have to be correlated to the polymerization changes analysed by Raman and ^{29}Si NMR experiments. The measured shift of the 50x-100Li ^{29}Si line can be interpreted in terms of polymerization and/or Si-O-Si average angle evolution. According to literature [16], an Si-O-Si angle decrease gives rise to a higher ^{29}Si chemical shift. In contrast, a much greater polymerization leads to a ^{29}Si line shifted to the lower chemical shift. We previously showed by Raman spectroscopy that the average Si-O-Si angle decreases in irradiated glasses, implying a shift of ^{29}Si line towards the higher chemical shift [11]. As a conclusion, the

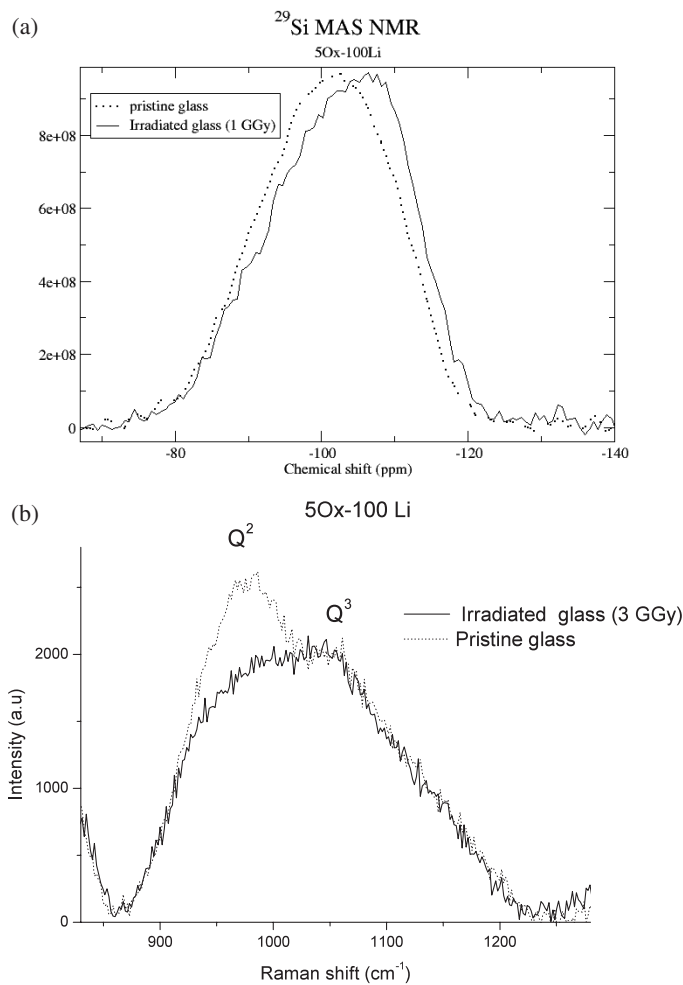


Figure 7. (a) ^{29}Si MAS NMR spectra of 50x–100Li irradiated and non-irradiated glasses. (b) Raman spectra of 50x–100Li irradiated and non-irradiated glasses.

lower chemical shift of the ^{29}Si line in Li irradiated glass can be interpreted as a significant polymerization increase. This result is perfectly consistent with the Raman measurements showing an important Q^3/Q^2 increase in the Li-irradiated glass. It is thus important to notice that the Q^3/Q^2 ratio in that case can be assimilated to the glass polymerization (Raman measurements are weakly sensitive to Q^4 species). All glasses show an important Q^3/Q^2 increase except in the 50x–50Li composition where polymerization remains unchanged after irradiation. In both Na/Li and Na/K intermediate compositions, the molecular oxygen amount is under the Raman detection limits. The first conclusion obtained from the NMR and Raman results is that both processes (polymerization increase and boron conversion) are needed to produce enough molecular oxygen to be detected by Raman spectroscopy.

However, the absence of oxygen in the 50x–100K was observed while polymerization is attested as well as boron conversion (even low). One possible explanation is that molecular oxygen escapes from the sample by percolation channels used by alkali. We have demonstrated elsewhere [19] that molecular oxygen is concentrated near the glass surface, which supports

this interpretation. We can suppose moreover that the diffusion pathway may be linked to the alkali size, which could explain why molecular oxygen was detected in Na and Li, irradiated glasses [12].

4.2. Network modification

Another interesting point to be underlined is that structural modifications under irradiation depend on which alkali type is mixed in glass. The best example is that the MAE is able to block either alkali in the network modifier position (Na/Li glass) or in the charge compensator position and more particularly those linked to BO_4^- entities (Na/K glass). However, we show that for 1 GGy dose, the aluminium fourfold coordination is stable under irradiation whatever the glass composition. We may wonder if the differences between 5Ox–50Li and 5Ox–50K concerning boron coordination stability under irradiation can be connected to the initial BO_4/BO_3 ratio in pristine glass. We showed in [15] that the BO_4/BO_3 ratio is much more important for 5Ox–50Li than 5Ox–50K glass, suggesting a higher amount of tetrahedral boron available to be converted. The origin of differences between both series is rather linked to the alkali repartition in the matrix. Hence, we demonstrated (figure 5) that in the Na/K series, Na^+ cations could play the role of AlO_4^- preferential charge balancing cations. It is worth mentioning that about 30% of total alkalis are concerned with the AlO_4^- charge equilibrium. This structural feature implies a different alkali repartition as modifier and BO_4^- charge compensator in the Na/K series than in the Na/Li series. It is however difficult to propose a precise quantitative repartition of alkalis in both glass series. ^{11}B – ^{23}Na SEDOR (spin echo double-resonance) NMR experiments will soon bring information about alkalis linked to the boron network.

Another question concerns the stabilization of boron under the tetrahedral environment. The conversion ability is connected to the facility for the alkali charge balancing cation to migrate. We showed that conversion is a little more efficient for Li than Na than K. This result is consistent with other structural changes like point defect creation or polymerization changes reported in [12]. If we now analyse the NMR BO_4 line shape variation, it remained the same after irradiation except in the 5Ox–100K glass (figure 2). Concerning this composition, we previously showed by Raman spectroscopy that danburite type rings (composed of two BO_4 and two SiO_4 tetrahedra) in this glass are much more numerous [15]. The BO_4 shape evolution of 5Ox–100K is characterized by the decrease of the -2 ppm component that could be interpreted as a danburite ring type decrease with regard to our last work [15]. This result can be supported by Raman considerations: the narrow band at 630 cm^{-1} corresponds to the vibration mode of rings composed of two BO_4 and two SiO_4 tetrahedra similar to the danburite mineral [15]. We can see in figure 8 that the 630 cm^{-1} band intensity decreases after irradiation in 5Ox–100K glass. This attests that fewer danburite-type rings participate in the glass structure after irradiation. In other terms, this result implies the (B, Si) ring conversion due to the K migration in the vicinity of danburite type rings.

Concerning irradiated compositions and aluminium environment, a general trend is observed: β irradiation causes an increase of the FWHM of the ^{27}Al band. The slight increase of FWHM can be either due to the interaction of paramagnetic point defects created under radiation [12] or to an increase of the quadrupolar interaction distribution. In order to interpret more precisely those changes, MQ-MAS spectra were recorded. The MQ-MAS spectrum of the 100 K irradiated glass exhibits a broadening along the quadrupolar interaction shift distribution line as shown in figure 9 whereas no significant change is visible along the chemical shift distribution direction. This result confirms the trend observed on the MAS spectrum (figure 2), that is a P_Q increase under β irradiation. So it can be concluded that paramagnetic defects do not strongly influence the line shape of the ^{27}Al irradiated glasses and the observed

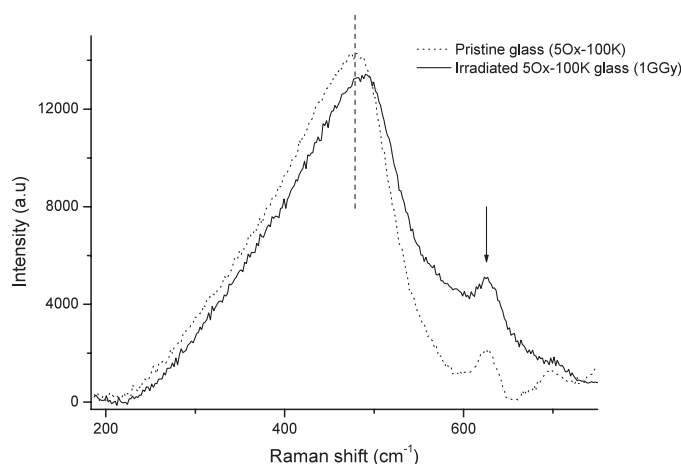


Figure 8. Raman spectra of 50x–100K irradiated and non-irradiated glasses in the 200–750 cm^{-1} range.

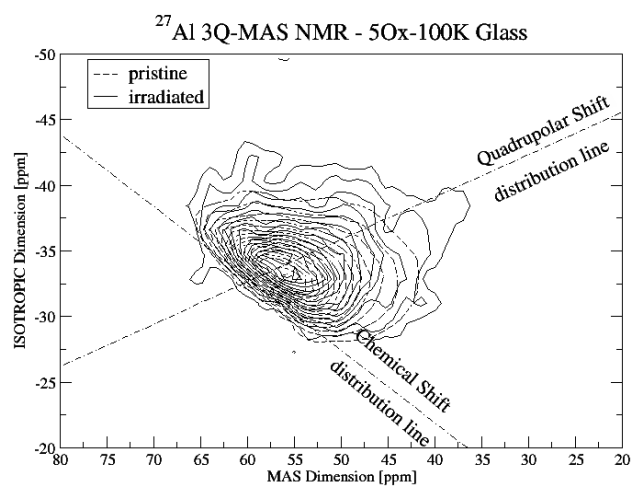


Figure 9. ^{27}Al 3MQ-MAS spectra of the 50x–100K irradiated and pristine glass.

FWHM of MAS spectrum increase can be mainly assimilated to an Al environment change under irradiation (probably a distortion).

5. Conclusion

We analyse glass structure evolution under irradiation and especially we examine the mixed alkali effect on alkali migration under irradiation. ^{11}B , ^{29}Si , ^{27}Al NMR experiments allow us to determine subtle behaviour differences between glasses depending on the alkali nature. A fourfold aluminium coordination is maintained under irradiation; however, the aluminium environment appears to be less ordered in all irradiated samples. More precisely, we show that in 50/50 Na/Li irradiated glass polymerization is stable, whereas BO_4 conversion into BO_3 species occurs. An opposite trend is observed in the 50/50 Na/K glass where boron conversion is absent and polymerization increase takes place. Each specific intermediate

irradiated composition leads to the formation of a low quantity of molecular oxygen (not detected by Raman spectroscopy; see [12]).

This difference of behaviour concerning the selective blockage of modifier or charge compensator alkalis could be explained from a different alkali repartition in both glass series based on a Na preferential $[\text{AlO}_4^-]$ charge compensating role in the Na/K series.

Anyway, we demonstrate that by changing the glass composition and using the mixed alkali effect, we were able to notably decrease the structural evolutions under irradiation.

Acknowledgments

The authors are indebted to T Pouthier and S Esnouf for the irradiation procedure preparation. We also thank V Métayer for x-ray diffraction measurements. Thank you to Gilles Montagnac for Raman experiments.

References

- [1] Ewing R C, Weber W J and Clinard F W 1995 *Prog. Nucl. Energy* **29** 63
- [2] Weber W J 1988 *Nucl. Instrum. Methods Phys. Res. B* **32** 471
- [3] Antonini M 1985 *J. Phys. Chem. Solids* **46** 287
- [4] DeNatale J F and Howitt D G 1984 *Nucl. Instrum. Methods Phys. Res. B* **1** 489
- [5] Sun K, Wang L M, Ewing R C and Weber W J 2004 *Nucl. Instrum. Methods Phys. Res. B* **218** 368
- [6] Boizot B, Petite G, Ghaleb D, Pellerin N, Fayon F, Reynard B and Calas G 2000 *Nucl. Instrum. Methods Phys. Res. B* **166/167** 500
- [7] Ollier N, Champagnon B, Boizot B, Guyot Y, Panczer G and Padlyak B 2003 *J. Non-Cryst. Solids* **323** 200
- [8] Olivier F, Boizot B, Ghaleb D and Petite G 2004 *J. Non-Cryst. Solids* at press
- [9] Mogus-Milankovic A, Santic B, Day D E and Ray C S 2001 *J. Non-Cryst. Solids* **283** 119
- [10] Ghosh S and Ghosh A 2002 *Solid State Ion.* **149** 67
- [11] Balaya P and Sunandana C S 1994 *J. Non-Cryst. Solids* **175** 51
- [12] Ollier N, Boizot B, Reynard B, Ghaleb D and Petite G 2004 *Nucl. Instrum. Methods B* **218** 176
- [13] Amoureux J P, Fernandez C and Steuernagel S 1996 *J. Magn. Reson.* **123** 16
- [14] Bunker B C, Tallant D R, Turner G L and Kirkpatrick R J 1990 *Phys. Chem. Glasses* **31** 30
- [15] Ollier N, Charpentier T, Boizot B, Wallez G and Ghaleb D 2004 *J. Non-Cryst. Solids* **341** 26
- [16] Engelhardt G and Michel D 1987 *High-Resolution Solid State NMR of Silicates and Zeolites* (New York: Wiley)
- [17] Ratai E J M and Eckert H 1998 *Solid State Ion.* **105** 37
- [18] Mc Millan P 1984 *Am. Miner.* **69** 622
- [19] Ollier N, Boizot B, Reynard B, Ghaleb D and Petite G 2004 *J. Nucl. Mater.* at press